Dynamics simulation of a π-conjugated light-harvesting dendrimer II: phenylene-based dendrimer (phDG2)

Dynamics simulation of a π-conjugated light-harvesting dendrimer II: phenylene-based dendrimer (phDG2)

Yasunobu Kodama, Soh Ishii and Kaoru Ohno

Department of Physics, Yokohama National University, 79-5 Tokiwadai, Hodogaya-ku, Yokohama 240-8501, Japan

Abstract
We investigate the light-harvesting property of a π-conjugated dendrimer, phenylene-based dendrimer (phDG2), by carrying out a semi-classical Ehrenfest dynamics simulation based on the time-dependent density functional theory. Similar to our previous study of star-shaped stilbenoid phthalocyanine (SSS1Pc), phDG2 shows electron and hole transfer from the periphery to the core through a π-conjugated network when an electron is selectively excited in the periphery. The one-way electron and hole transfer occurs more easily in dendrimers with planar structure than in those with steric hindrance because π-conjugation is well maintained in the planar structure. The present results explain recent experiments by Akai *et al* (2005 *J. Lumin.* **112** 449).

(Some figures in this article are in colour only in the electronic version)

1. Introduction

Dendrimers are nanometer-scale organic molecules with dendritic structures. In the so-called light-harvesting dendrimers, the optical energy absorbed in the periphery is transferred to the core, and a significant amount of energy can be concentrated at the core [1, 2]. These special dendrimers have attracted considerable interest because of their potential for future nanotechnological applications.

In our previous study, we performed a semi-classical Ehrenfest dynamics simulation of a π-conjugated small dendrimer, star-shaped stilbenoid phthalocyanine (SSS1Pc) [3], by using the local density approximation of the time-dependent density functional theory [4]. We will refer to this previous paper [4] as I. We found that the one-way electron and hole transfer occurs from periphery to core, i.e. the light-harvesting property exists in this dendrimer. As demonstrated in I, the mechanism of the one-way electron and hole transfer is related to the relative position of the energy gap of the periphery and core analogous to the mechanism of the p–n junction in semiconductors. It is summarized as follows. If the energy gap of the periphery is larger than and surrounding the energy gap of the core in the absolute positions of the energy levels, an electron excited in the periphery automatically moves toward the lower empty level in the core, and a hole created in the

periphery automatically moves toward the higher occupied level in the core. In addition, we found that the electron and hole transfer occurs more easily in dendrimers with planar structure than in those with steric hindrance, because π-conjugation is well maintained in a planar structure. The results well explain the recent experiment performed by Akai *et al* [5].

In the present paper, we investigate the energy transfer in a different phenylene-based dendrimer (phDG2) [6], which was also experimentally studied by Akai *et al* [5]. The time-dependent part of our calculation is based on an all-electron mixed basis approach which has been developed in our group[1]. In this method, the wavefunction is expanded in linear combination of both atomic orbitals and plane waves. So far, this method has been used for various applications such as foreign atom insertions into C_{60} [8], GW calculations for clusters and solids [9], and T-matrix calculations [10]. Here again, we investigate the relation between the energy transfer and the structure of dendrimers.

Now, we consider the phDG2 with one periphery, which we call phDG2-1, and that with two peripheries, which we call phDG2-2. The optimized structure of phDG2-1

---

[1] The original all-electron mixed basis program used in this paper is that first developed by K Ohno. This approach is briefly explained in [7].

(a)

(b)
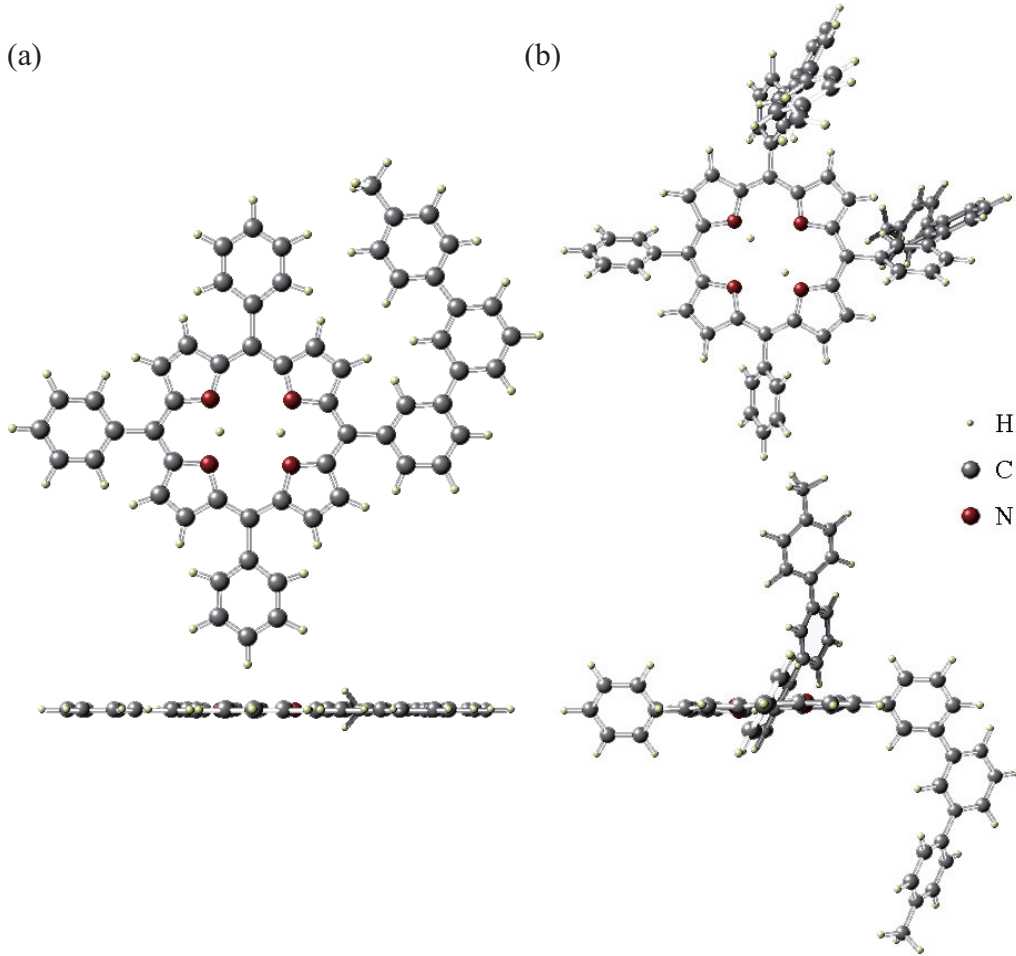
Figure 1. Structure of (a) phDG2-1 and (b) phDG2-2. In both (a) and (b), upper figures show the front view and lower figures show the side view. The structure of phDG2-2 (b) is three-dimensional due to steric hindrance between the peripheries.

obtained by using the Gaussian 03 package [11] is two-dimensional (figure 1(a)) and that of phDG2-2 is three-dimensional (figure 1(b)) due to the steric hindrance between the peripheries. Below, as well as in our previous paper, I, of SSS1Pc [4], we will show that the energy transfer is suppressed by the steric hindrance between the peripheries of phDG2-2. This result again explains the experimental behavior that the efficiency of the electron and hole transfer increases with the temperature, because the periphery and the core come more frequently in the same plane instantaneously due to torsional vibration.

In this work, we perform a semi-classical Ehrenfest dynamics simulation similar to our previous studies [4, 15]. We use the time-dependent local density approximation (TDLDA), i.e. the adiabatic LDA [12] of the time-dependent density functional theory (TDDFT) for electrons [13] and the Newtonian equation of motion for nuclei. The method is essentially the same as that adopted in I.

2. Methodology

The time-dependent Kohn–Sham (TDKS) equation within the TDLDA [14] is given by

$$i\hbar(\partial/\partial t)\psi_j(\boldsymbol{r}, t) = H(t)\psi_j(\boldsymbol{r}, t), \tag{1}$$

where $H(t)$ is the electronic part of the Hamiltonian and $\psi_j(\boldsymbol{r}, t)$ denotes the wavepacket of the jth level. We use the spectral method to accurately integrate the TDKS equation with respect to time [15, 16]. In this method, we use the eigenstates and eigenvalues that satisfy $H(t)\phi_k(\boldsymbol{r}, t) = \epsilon_k(t)\phi_k(\boldsymbol{r}, t)$. The wavepackets $\psi_j(\boldsymbol{r}, t)$ are expanded in terms of the eigenstates as

$$\psi_j(\boldsymbol{r}, t) = \sum_k c_{jk}(t)\phi_k(\boldsymbol{r}, t). \tag{2}$$

Within the time interval Δt in which the Hamiltonian does not change at least approximately, we can integrate the TDKS equation as

$$\psi_j(\boldsymbol{r}, t + \Delta t) = \sum_k \exp[-i\epsilon_k(t)\Delta t]c_{jk}(t)\phi_k(\boldsymbol{r}, t). \tag{3}$$

In what follows, we use the all-electron mixed basis approach [15, 16] in which $\psi_j(\boldsymbol{r}, t)$ and $\phi_k(\boldsymbol{r}, t)$ are expressed as linear combinations of both (numerical) atomic orbitals (AOs) and plane waves (PWs). We use 345 and 420 AOs, respectively, for phDG2-1 and phDG2-2, and 24405 PWs corresponding to the cutoff energy of 7.0 Ryd for both phDG2-1 and phDG2-2. In contrast to the usual LCAO approaches, this basis can almost span the entire space of the system as required in the spectral method.
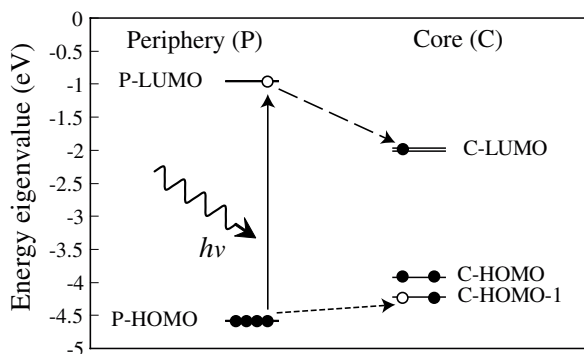
Figure 2. The energy eigenvalues of phDG2-2. Black and white circles denote electrons and holes, respectively. After an electron is excited from the (almost doubly degenerate) P-HOMO levels to the (doubly degenerate) P-LUMO levels on the periphery side (solid line with an arrow), the electron is transferred from the P-LUMO levels to the (doubly degenerate) C-LUMO levels (dashed line with an arrow), and the hole is transferred from the P-HOMO levels to the C-HOMO level (dotted line with an arrow).

3. Results

The calculated energy levels and wavefunctions at the ground state of phDG2-2 are shown in figures 2 and 3, respectively. Here, it is convenient to distinguish between the levels associated with the core (C) and those associated with the periphery (P) because the wavefunctions in P and C are almost separated in space, as shown in figure 3. The wavefunctions of the highest occupied molecular orbital (HOMO) level and the doubly degenerate lowest unoccupied molecular orbital (LUMO), LUMO + 1 levels are spread over the C region. Therefore, we refer to the HOMO level as the C-HOMO level, and the LUMO, LUMO + 1 levels as C-LUMO levels. Similarly, the wavefunctions of the almost doubly degenerate HOMO-2, HOMO-1 levels and the doubly degenerate LUMO + 2, LUMO + 3 levels are spread only

over P, and they are termed P-HOMO and P-LUMO levels, respectively. The ground-state electronic structure of phDG2-1 is similar to that of phDG2-2. The only difference between phDG2-1 and phDG2-2 is that both P-HOMO and P-LUMO levels are nondegenerate in phDG2-1 and doubly degenerate in phDG2-2. This is because phDG2-1 has one peripheral group, while phDG2-2 has two peripheral groups of the same molecule. When the periphery absorbs light, an electron is excited from the P-HOMO level to the P-LUMO level. Since the stability of the electron (hole) increases with decreasing (increasing) energy, one-way energy transfer occurs from the periphery to the core.

For the dynamics, we perform a time-dependent simulation of the electron and hole transfer from the periphery to the core of phDG2-1 and phDG2-2 after exciting an electron from the P-HOMO level to the P-LUMO level. The initial electronic states are self-consistently determined on the adiabatic surface of the optically excited state, and therefore include the exciton configuration and the related long-range interaction beyond linear response [17]. The TDKS equation for electrons coupled with the Newtonian equation of motion for nuclei is integrated stepwise with the basic time step $\Delta t = 0.25$ fs. Total energy including the electronic part, the potential energy between nuclei, and the kinetic energy of nuclei is conserved in this simulation.

First of all, if we fix the position of nuclei during simulation, nothing happens in the electronic states, because the initial electronic states are the steady state solutions of the TDKS equation[2]. However, if we relax the constraint of the atomic positions, the excited electron tends to transfer from the periphery to the core in the wavepacket of the P-LUMO level,

---

[2] In the case of the dendrimers, SSS1Pc and phDG2, the difference in the energy eigenvalues between the periphery-LUMO and core-LUMO levels is large, and there is no level mixing in the simulation with fixed atomic positions. However, we note that, in figure 3 of [14], the difference in the energy eigenvalues between the CH4-LUMO and Li2-LUMO levels is small, and the two eigenstates can be slightly mixed even when atomic positions are fixed in the CH4-Li2 system.
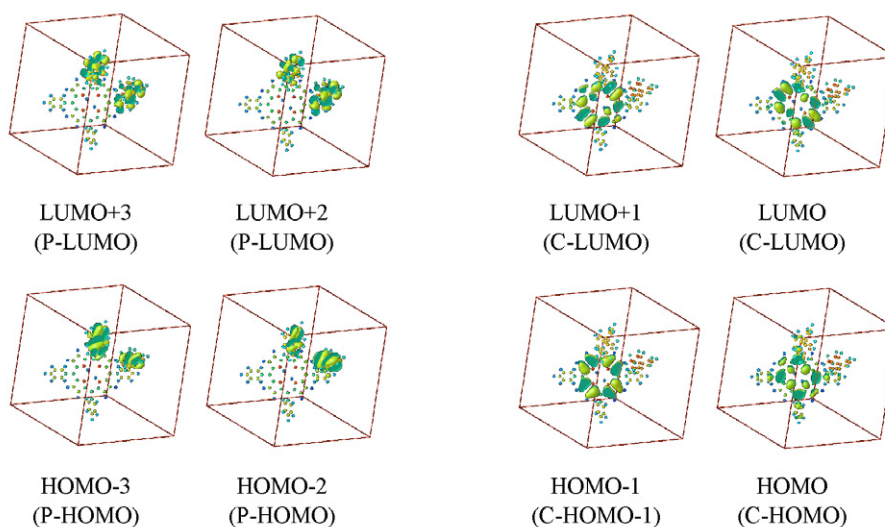
Figure 3. Amplitude of the wavefunctions at the ground state of phDG2-2. The cubes represent the unit cell. In each figure, the regions at the center and the upper right-hand side correspond to the core and the periphery, respectively. Bright and dark areas denote the positive and negative values of the wavefunction, respectively.
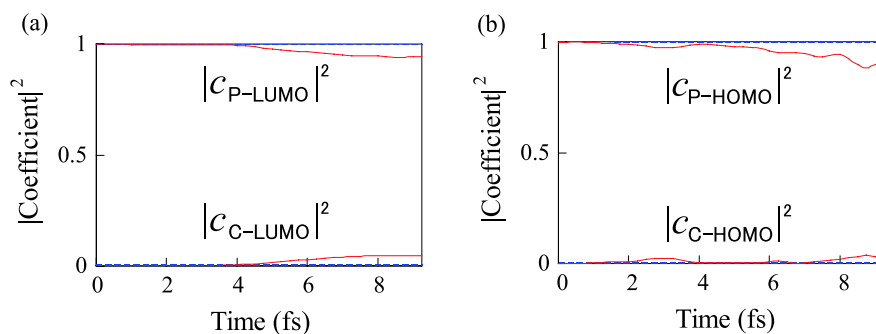
Figure 4. Time evolution of the absolute squared coefficients for the P- and C-eigenstates in the wavepacket of (a) the P-LUMO level and (b) the P-HOMO level. The upper (lower) curves correspond to the P-LUMO (C-LUMO) eigenstates for (a) and P-HOMO (C-HOMO-1) eigenstates for (b). The solid and dashed curves denote phDG2-1 and phDG2-2, respectively. The dashed curves are not visible because they are almost on the upper and lower horizontal axes.

$\psi_{\text{P-LUMO}}$. Similarly, in the wavepacket of the P-HOMO level, $\psi_{\text{P-HOMO}}$, the hole created by the electron excitation transfers from the periphery to the core. The details are as follows.

At $t = 0$, the wavepacket of the P-LUMO level, $\psi_{\text{P-LUMO}}$, coincides with the pure eigenstate, $\phi_{\text{P-LUMO}}$. At later times, it becomes a linear combination of the eigenstates of the P-LUMO and C-LUMO levels as $c_{\text{P-LUMO}}\phi_{\text{P-LUMO}} + c_{\text{C-LUMO}}\phi_{\text{C-LUMO}}$. Figure 4(a) represents the time evolution of the absolute square of the coefficients of the two eigenstates, $|c_{\text{P-LUMO}}|^2$ and $|c_{\text{C-LUMO}}|^2$, in the components of the P-LUMO wavepackets of phDG2-1 (solid curves) and phDG2-2 (dashed curves). The two eigenstates are mixed in the wavepacket of phDG2-1 after 4 fs. This implies that there exists a net probability of the electron transfer from the P-LUMO level to the C-LUMO level in phDG2-1. However, in the case of phDG2-2, the mixing is negligibly small. This is due to the steric hindrance in phDG2-2.

Similarly, the wavepacket of the P-HOMO level, $\psi_{\text{P-HOMO}}$, coincides with $\phi_{\text{P-HOMO}}$ at $t = 0$. At later times, it becomes a linear combination of the eigenstates of the P-HOMO and C-HOMO-1 levels as $c_{\text{P-HOMO}}\phi_{\text{P-HOMO}} + c_{\text{C-HOMO-1}}\phi_{\text{C-HOMO-1}}$. Figure 4(b) shows the time evolution of the absolute square of the coefficients of the two eigenstates, $|c_{\text{P-HOMO}}|^2$ and $|c_{\text{C-HOMO-1}}|^2$, in the components of the P-HOMO wavepackets of phDG2-1 (solid curves) and phDG2-2 (dashed curves). In the case of phDG2-2, the mixing is again negligibly small. This implies that the steric hindrance in phDG2-2 also interrupts the hole transfer. In the case of phDG2-1, the two eigenstates are slightly mixed in the wavepacket after 2 fs. Compared with the value of the difference between $|c(t > 0)|^2$ and $|c(t = 0)|^2$, $|c_{\text{P-HOMO}}(t > 0)|^2 - |c_{\text{P-HOMO}}(t = 0)|^2$, $|c_{\text{P-LUMO}}(t > 0)|^2 - |c_{\text{P-LUMO}}(t = 0)|^2$ is large. This is because $\phi_{\text{P-HOMO}}$ becomes $c_{\text{P-HOMO}}\phi_{\text{P-HOMO}} + c_{\text{C-HOMO-1}}\phi_{\text{C-HOMO-1}} + c_{\text{C-HOMO-2}}\phi_{\text{C-HOMO-2}}$.

4. Discussion

From these results, we find that the one-way electron and hole transfer separately occurs from the periphery to the core of phDG2 similar to the system (SSS1Pc) investigated in I. The

probability of the electron and hole transfer is obviously much higher in phDG2-1 than in phDG2-2. This result strongly suggests that the electron and hole transfer is caused by the π-conjugation and is suppressed by the steric hindrance of molecular structure. That is, the efficiency of the energy transfer depends on the steric hindrance of molecular structure in accordance with the experiments [5] in a sense that the electron and hole transfer is caused by π-conjugation. This main conclusion and the following discussions are mostly the same as our previous paper, I, on SSS1Pc [4].

Figures 5(a) and (b) show the energy eigenvalues (solid curves) and the energy expectation values (dashed curves) of the P-LUMO and C-LUMO levels of phDG2-1 and phDG2-2, respectively. First of all, we note that the energy eigenvalues and the energy expectation values change smoothly and ΔE is $\sim$0.1 eV at its largest, which suggests that there is no rapid change in the electronic density and the present TDLDA treatment is valid. We also find that the net probability of the electron transfer increases when the difference between the energy eigenvalues and the energy expectation values, $\Delta E = |\varepsilon_k - \langle \psi_k | H | \psi_k \rangle|$, increases, where $|\psi_k\rangle$ is the wavepacket. One may also see that the net probability of the electron transfer increases when the eigenvalues of the P-LUMO (black curves) and C-LUMO (gray curves) levels approach each other. These behaviors are explained by the mixing of the states when the electron transfer takes place from the periphery to the core.

Similarly, figures 5(c) and (d) show the energy eigenvalues and energy expectation values of the P-HOMO and C-HOMO-1 levels of phDG2-1 and phDG2-2, respectively. In this case also, the net probability of the hole transfer increases, when the difference ΔE between the energy eigenvalues and the energy expectation values increases. Again, these figures show that the energy eigenvalues and the energy expectation values change smoothly and ΔE is $\sim$0.1 eV at its largest. Therefore, there is no rapid change in the electronic density and the present TDLDA treatment is valid.

During the simulation, the average distance between hydrogen atoms and carbon atoms very slightly increases by 0.078 Å in phDG2-1 and by 0.085 Å in phDG2-2 in 9.25 fs. Within this short time interval, the structures of phDG2-1 and phDG2-2 do not vibrate, but each atom moves unidirectionally. Thus, we clearly observed that such a very small atomic motion
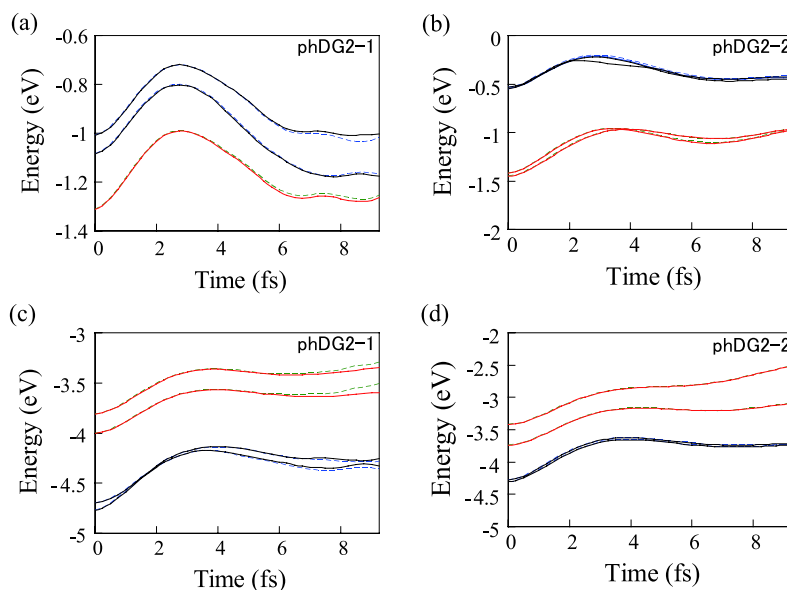
Figure 5. Time evolution of the energy eigenvalues (solid curves) and energy expectation values (dashed curves). (a) and (b) show the P-LUMO (black curves) and C-LUMO (gray curves) levels of phDG2-1 and phDG2-2, respectively. (c) and (d) show the P-HOMO (black curves) and C-HOMO-1 (gray curves) levels of phDG2-1 and phDG2-2, respectively.
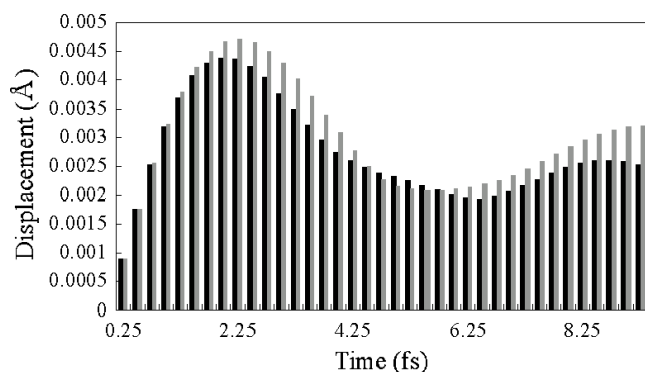
Figure 6. Time evolution of the mean displacement during Δt (i.e. the mean velocity) of the average of all atoms ($\sum_i^N |r_i(t) - r_i(t - \Delta t)|)/N$. The black and gray bars show the phDG2-1 and phDG2-2, respectively.

can induce electron and hole transfer. Moreover, figure 6 shows the time evolution of the mean displacement during Δt of all atoms ($\sum_i^N |r_i(t) - r_i(t - \Delta t)|)/N$. From figures 5 and 6, we find that when the energy eigenvalues and the energy expectation values change by a comparatively large amount in time, the mean displacement (or the mean velocity) becomes large.

The dendrimer having two arms shown in figure 1(b) has two hydrogen atoms associated with two of the four nitrogen atoms around the center. The remaining two nitrogen atoms are not attached to hydrogen atoms. In contrast, in the dendrimer having one arm (figure 1(a)), each hydrogen atom is located in the middle of two nitrogen atoms. These structures were determined by geometrical optimization with Gaussian03. The maximum value of the remaining force acting on atoms was 0.00024 Hartree/bohr ($\sim$0.01 eV/Å^{-1}) after optimization. A

vibrational frequency analysis was not made, so this stationary point structure is not guaranteed to be a minimum. A simple calculation shows that hydrogen atoms move 0.004 Å at the maximum time step in our simulation ($\sim$9 fs). This small movement of the hydrogen atoms at the core does not affect our final result. In the excited state dynamics, we found that the mean atomic displacement during the simulation time period is about 0.08 Å. This value is much larger than the above value (0.004 Å) of the possible displacement of hydrogen atoms in the ground state. In this sense, we believe that the optimized geometry of the dendrimers at the ground state does not affect the dynamics at the excited state inaccurately.

However, for longer time scales, the atomic motion becomes large and the semi-classical Ehrenfest dynamics breaks down. Therefore, a more elaborated simulation such as surface hopping [18, 19] would be required in a future study.

5. Summary

In summary, by performing the first-principles molecular dynamics simulation using the TDKS equation on the basis of the TDDFT, we have investigated the light-harvesting mechanism of phDG2, when an electron is selectively excited in the periphery. We found that the one-way electron and hole transfer occurs from the periphery to the core through a π-conjugated network during a very slight motion of molecules. Moreover, by comparing two structures without and with steric hindrance of these dendrimers (phDG2-1 and 2), we found that the electron and hole transfer occurs more easily in dendrimers with a planar structure than in those with steric hindrance, because π-conjugation is well maintained in the planar structure. The present results explain well the recent experiment done by Akai *et al* [5]. These results are mostly the same as the results of our previous paper, I, for the light-harvesting property of a π-conjugated dendrimer, star-shaped

stilbenoid phthalocyanine (SSS1Pc) [4], and therefore we conclude that the results are universal among these molecules.

Acknowledgments

References

[1] Devadoss C, Bharathi P and Moore J S 1996 *J. Am. Chem. Soc.* **118** 9635
[2] Nakano M, Takahata M, Yamada S, Kishi R, Nitta T and Yamaguchi K 2004 *J. Chem. Phys.* **120** 2359
[3] Kimura M, Narikawa H, Ohta K, Hanabusa K, Shirai H and Kobayashi N 2002 *Chem. Mater.* **14** 2711
[4] Kodama Y, Ishii S and Ohno K 2007 *J. Phys.: Condens. Matter* **19** 365242
[5] Akai I, Nakao H, Kanemoto K, Karasawa T, Hashimoto H and Kimura M 2005 *J. Lumin.* **112** 449
[6] Kimura M, Shiba T, Yamazaki M, Hanabusa K, Shirai H and Kobayashi N 2001 *J. Am. Chem. Soc.* **123** 5636
[7] Ohno K, Esfarjani K and Kawazoe Y 1999 *Computational Materials Science: from Ab Initio to Monte Carlo Methods* (*Springer Series in Solid-State Sciences* vol 129) (Berlin: Springer) pp 39–46, 68 and 95
[8] Ohtsuki T, Ohno K, Shiga K, Kawazoe Y, Maruyama Y and Masumoto K 1998 *Phys. Rev. Lett.* **81** 967
[9] Kikuchi E, Iwata S, Ishii S and Ohno K 2007 *Phys. Rev.* B **76** 075325
[10] Ohno K, Noguchi Y, Yokoi T, Ishii S, Takeda J and Furuya M 2006 *ChemPhysChem* **7** 1820
[11] *GAUSSIAN 03* 2004 (Wallingford, CT: Gaussian Inc.)
[12] Vignale G and Kohn W 1996 *Phys. Rev. Lett.* **77** 2037
[13] Runge E and Gross E K U 1984 *Phys. Rev. Lett.* **52** 997
[14] Marques M A L, Ullrich C A, Nogueira F, Rubio A, Burke K and Gross E K U 2006 *Time-Dependent Density Functional Theory* (Berlin: Springer)
[15] Kodama Y and Ohno K 2006 *J. Chem. Phys.* **125** 054501
[16] Sawada T and Ohno K 2005 *Chem. Phys. Lett.* **405** 234
[17] Ohno K 2007 *Mater. Trans.* **48** 649
[18] Tapavicza E, Tavernelli I and Rothlisberger U 2007 *Phys. Rev. Lett.* **98** 023001
[19] Werner U, Mitric R, Suzuki T and Bonacic-Koutecky V 2008 *Chem. Phys.* **349** 319